Primljen / Received: 7.4.2023.
Ispravljen / Corrected: 15.6.2023.
Prihvaćen / Accepted: 4.8.2023.
Dostupno online / Available online: 10.11.2023.

Nonlinear behaviour of liquefied natural gas tanks with different seismic isolation systems

Authors:

İbrahim Hüner, PhD. CE
Pamukkale University, Denizli, Turkey
Department of Civil Engineering
fsm-1453@hotmail.com
Corresponding author

Prof. **Bülent Akbaş**, PhD. CE
Gebze Institute of Technology, Gebze, Kocaeli, Turkey
Department of Civil Engineering
akbasb@gyte.edu.tr

Prof. **Abdullah Cem Koç**, PhD. CE
Pamukkale University, Denizli, Turkey
Department of Civil Engineering
a_c_koc@pau.edu.tr

Research Paper

İbrahim Hüner, Bülent Akbaş, Abdullah Cem Koç

Nonlinear behaviour of liquefied natural gas tanks with different seismic isolation systems

This study determines the effects of different types of base isolator systems on the seismic performance of liquefied natural gas (LNG) storage tanks. Nonlinear time-history analyses of the non-isolated and three different isolated models were performed for the average acceleration of seven ground motions scaled to achieve a specified safe shutdown earthquake. The ANSYS Workbench program was used in the modelling studies of the LNG liquid, inner steel tank, outer shell, ring beam, roof and concrete foundation and side wall insulation. The LS-DYNA program was used for the nonlinear analyses of the LNG liquid, inner steel tank and concrete foundation. The results of the total base shear force, sloshing height, steel tank stresses and lateral deflection were compared. The results indicated that there was no difference between the convective and impulsive modes for the LNG tanks with isolators. It was concluded that the wave motion of the liquid was different from the oscillation of the structure and the earthquake isolation times did not affect the sloshing motion. In the non-isolated system, the stress reached 400 MPa, whereas it was 350 MPa on average in the LNG tanks with isolators.

Key words:
liquefied natural gas tanks, HDRB, LRB, FPS, LS-DYNA, ANSYS workbench, nonlinear analyses

Prethodno priopćenje

İbrahim Hüner, Bülent Akbaş, Abdullah Cem Koç

Nelinearno ponašanje spremnika za ukapljeni prirodni plin s različitim sustavima potresne izolacije

Ovaj rad pobliže određuje učinke različitih tipova izolacijskih sustava na ponašanje spremnika za ukapljeni prirodni plin (engl. *liquefied natural gas* - LNG) tijekom potresa. Provedene su nelinearne analize primjenom vremenskog zapisa neizoliranih i triju različitih izoliranih modela za prosječno ubrzanje sedam vrsta gibanja tala stupnjevanih kako bi se postigla određena moguća sigurna obustava rada postrojenja tijekom potresa. Program ANSYS Workbench primijenjen je za modeliranje tekućine ukapljenog plina, unutarnjeg čeličnog spremnika, vanjske stijenke, serklaže, krova, betonskih temelja i izolacije stražnje stijenke. Program LS-DYNA primijenjen je za nelinearne analize tekućine LNG-a, unutarnjeg čeličnog spremnika i betonskih temelja. Uspoređeni su rezultati ukupne poprečne potresne sile u podnožju, visine zapljuskivanja, naprezanja čeličnog spremnika i bočnog pomaka. Rezultati su pokazali da nema razlike između konvektivnih i impulsnih modova za izolirane spremnike LNG-a. Zaključeno je da se valno gibanje tekućine razlikuje od osciliranja konstrukcije, a razdoblja protupotresnih izolacija nisu utjecala na zapljuskivanje. U neizoliranom su sustavu vrijednosti naprezanja dosegle 400 MPa, dok su te vrijednosti u izoliranim spremnicima za LNG prosječno iznosile 350 MPa.

Ključne riječi:
spremnik za ukapljeni prirodni plin, gumeni ležajevi s velikim prigušenjem (HDRB), gumeni ležajevi s olovnom jezgrom (LRB), klizni ležajevi s njihalom (FPS), nelinearne analize

1. Introduction

Natural gas is a hydrocarbon-based gas that consists largely of methane and has a very low density (0.66 kg/m³). The transportation of natural gas, which plays an important role in meeting the energy demands of the world, from source to end user, is a critical process. Road transport has become an important alternative to natural gas supply owing to problems such as natural disasters and security issues in natural gas transmission lines located at sea and on land. Liquefied natural gas (LNG) (430–480 kg/m³) is used in land and sea transportation and it is obtained by the condensation of natural gas at –168 °C temperature and normal atmospheric pressure conditions. It should be noted that there is a difference of approximately 600 times between the densities of liquid natural gas and gaseous gas. Different types of storage and transport tanks are used to provide reasonably fast and predictable transportation of LNG. These tanks are generally divided into different classes, such as heavy-tonnage pickup truck, ship, terminal and storage tanks [1]. The tank type covered in this study is the fixed LNG storage tank with very large storage volume. These tanks, which are called fully contained storage tanks, consist of an inner tank made of cryogenic steel (9 % nickel) and an outer cylindrical shell wall made of typical post-tensioned reinforced concrete along the vertical and radial directions. The base slab and spherical roof dome are made of reinforced concrete. Adequate thermal insulation is provided between the tanks [2]. In the more common cases, where the sole plate is in direct contact with the ground, freezing is prevented using electric heating plates [1].

In API 620 [3], API625 [4] and NFPA 59A [5], the design requirements for LNG tanks are stringent because they store a high-energy chemical substance. LNG storage tanks are designed according to three levels of seismic action. The operational basis earthquake (OBE) ground motion is represented by an acceleration response spectrum with a 10 % probability of exceedance over a 50 years period (mean return interval of 475 years). The tank system should be designed to continue operating during and after the OBE. After a safe shutdown earthquake (SSE), no deformation should occur in the tank support systems, insulation layers, or isolators. The accepted maximum considered earthquake (MCER), determined based on site-specific research, has a 2 % probability of exceedance within a 50 years period (mean recurrence interval of 2475 years). The aftershock level earthquake (ALE) ground motion is defined as half the SSE. An LNG tank system subjected to an ALE should maintain the primary container volume at its maximum operating level with no loss from the secondary container [3-5].

The behaviour of structures exposed to fluid pressure caused by earthquakes was first investigated by Westergaard in 1933 [6]. In the studies carried out by Jacobsen [7, 8], the rigid tank containing the liquid and the support legs carrying the horizontally accelerated liquid tank were analysed. In studies conducted by Housner [9, 10], the hydrodynamic pressure created by the liquid in the tank was separated into its components and the effects of the impulsive pressure caused by the liquid part accelerating with the tank and the convective pressure caused by the agitated liquid part were investigated. The convective component was then modelled using a single degree-of-freedom (DOF) oscillator [11, 12]. Haroun and Housner [13] developed a 3-DOF model for ground-supported deformable tanks, including flexible behaviour. Veletsos and Tang [14] also conducted similar studies. Malhatro et al. [15] considered the pulsed and convective modes and modified the properties of the mechanical analogue to include higher modes in the resulting base shear and base overturning moments.

The seismic risks of LNG storage tanks are higher than those of traditional buildings because they can lead to secondary disasters such as explosions and environmental pollution, which would result in significant property damage or loss of life. For example, the destruction of an LNG tank during the 1964 Niigata earthquake in Japan caused fires and explosions, resulting in serious societal losses and pollution [16]. Since the 1990s, several studies have been conducted on the dynamic analysis of LNG storage tanks [17, 18]. Basic isolation techniques, such as lead-core rubber bearings (LRBs), high-damping rubber bearings (HDRBs), steel hysteretic shock absorbers and friction pendulum bearings are used in the seismic design of LNG tanks and in many other applications in modern structural design [19-22]. Three different LNG tank structural configurations, that is, with a fixed bottom, seismically isolated with rubber bearings only and seismically isolated with rubber bearings and steel hysteretic dampers, were tested in [19]. The test results confirmed that the use of steel hysteretic dampers drastically decreased large displacements. Christovasilis and Whittaker [23] investigated the seismic response of a conventional and isolated 150,000 m³ capacity vertical cylindrical LNG tank by applying finite element analysis to mechanical models. The base shear and overturning moment in the seismically isolated LNG tank were 10 %–15 % of the values computed for the conventional tank and the wave heights were unaffected by the use of a seismic isolation system. Gregoriou et al. [20, 21] analysed the seismic response of three typical LNG tanks isolated using high-damping rubber bearings and lead-core rubber bearings. As a result of these processes, problems related to the base shear force and deflection of the inner steel were reduced by approximately 70 %–60 %. However, an increase in the agitation height was observed compared to the non-isolated tank, especially in the case of high-damping rubber support insulation. Marti et al. [1] studied a typical modern LNG tank with a capacity of 160,000 m³ and they reported that seismically isolated tanks can be used when the design peak ground accelerations are in the range of approximately 0.30–0.90 g. Ruifu et al. [22] analysed the seismic response of

a vertical, cylindrical, extra-large and insulated LNG tank with a multiple friction pendulum system (MFPS). They presented statistically classified data, including pile shear, wave height, impulsive acceleration, convective acceleration and outer tank acceleration and showed that the isolation system could adapt perfectly to different liquid levels and was very effective in controlling the seismic response of extra-large LNG tanks. Datoli et al. [24] examined an LNG tank with a capacity of approximately 172,000 m³ during an earthquake of 7.1 Richter magnitude. They constructed a finite element model (FEM) model consisting of a flat anchored base and a cylindrical metal wall in contact with the LNG and reported that the fluid motion and fluid–structure interactions were responsible for a failure type known as the elephant's foot. Zhao et al. [25] investigated the effects of liquid filling rate and earthquake motion periods on the efficiency of a lead–rubber bearing system using the ABAQUS program. Zhao et al. [26] investigated the liquid filling ratio and earthquake motion periods to determine the efficiency of a lead–rubber bearing system using the general finite element code ABAQUS. They analysed a 160,000 m³ LNG prestressed storage tank for 12 earthquake waves under four site classes using stress distributions on the outer and inner tanks, as well as tip displacement and base shear. The maximum stress of the inner tank was greater than 500 MPa at the 100 % liquid level in all four site classes, creating significant safety hazards. Design optimisation and establishment of an early warning system are imperative for controlling high liquid levels. Barone and Sartori [27] investigated two elevated LNG tanks with a full working capacity of 10,130 m³ and 91 pieces of friction pendulum systems (FPSs) isolated at the Corsini port of Ravenna, Italy. In their experiments, they observed that a high lateral flexibility and a high friction coefficient effectively separated the motion of the ground from the structure and dissipated some of the seismic energy. Kilic et al. [28] studied the performance of one broad tank, one medium tank and one slender tank with two- and three-dimensional elastomeric bearings, which were isolated along only the horizontal direction and in both directions (horizontal and vertical), respectively, by performing nonlinear dynamic time history analyses. It was observed that 3D isolators provided more efficient results than 2D isolators. Chen et al. [29] performed shake table tests and numerical models of an LRB isolated LNG tank. Although the base shear force, overturning moment and acceleration spectra of the tank were significantly reduced, the displacement of the tank posed a danger to the piping system connected to the tank. Sharari et al. [30] examined a 160,000 m³ full containment LNG tank considering the soil structure and fluid–structure interactions while assessing the impacts of the depth of soil liquefaction on the performance of different components of the system. According to the nonlinear time history results, the seismic forces on the inner steel and outer reinforced concrete tank walls decreased as the liquefaction depth increased. However, increases in the lateral displacements, shear forces and bending moments of the pile head were observed. The positive effects of the isolators on the LNG tank in earthquakes of 0.4 g and above were compared. To calculate the sloshing height in the wide and high LNG tanks with a long period of 9.80 s, earthquakes with a minimum of 27 s and above were selected. The effects of the isolators on the sloshing height of the LNG liquid were investigated. The analysis results of medium and strong earthquakes in anchored and isolated LNG tanks were evaluated.

This paper presents a case study analysing the behaviour of an LNG tank without seismic isolation and with three different types of base seismic isolation.

2. Description and modelling of the liquefied natural gas (LNG) tank

For this study, an LNG tank with a volume of 232.000 m³ constructed for high-seismic hazard areas was selected. The effects of the insulation type on the spherical bottom slip, LNG sloshing wave height, lateral displacements on the steel tank wall, stresses in the tank and earthquake isolation force–displacement diagrams were investigated. In this LNG tank, the height-to-radius ratio is 1. The LNG tank consists of an inner layer, insulation layer and outer layer. The height of the inner and outer tanks is 45 m and their diameters are 84 and 88 m, respectively. The maximum height of the liquid is 42 m. The outer shell has a constant thickness (0.8 m along its height), whereas the thickness of the inner shell increases from top to bottom, from 12 to 32 mm. The space (1.20 m) between the two shells was filled with perlite to provide thermal insulation. While the outer shell was placed directly on a circular foundation slab (1.80 m), a layer of foam glass (0.70 m) was placed between the inner shell base and foundation slab for thermal insulation. Analyses were performed considering the geometric properties listed

Table 1. Material properties of the LNG tank

Description	**Young modulus E (MPa)** [MPa]	**Poisson ratio** ν	**Mass density** γ [kg/m³]
Inner steel	210000	0.30	7850
Concrete	37000	0.20	2500
LNG	2000	-	480
Perlite isolation	7500	-	240
Foam glass isolation	1200	-	150

Table 2. Geometric dimensions of the LNG tank

Description	Dimension
Height of inner steel tank	45.00 m
Diameter of inner steel tank	84.00 m
Thickness of inner steel tank wall	32 mm-12 mm
Inner steel tank bottom thickness	5 mm
Height of LNG	42.00 m
Height of outer concrete tank	61.00 m
Diameter of outer concrete tank	88.00 m
Wall thickness of outer concrete tank	0.80 m
Sphere thickness of outer concrete tank	0.40 m
Outer concrete wall with between inner steel tank perlite insulation thickness	1.20 m
Thickness of bottom base insulation (foam glass)	0.70 m
Thickness of foundation	1.80 m

in Table 1 and the material properties listed in Table 2. The steel tank forming the inner layer is composed of a nickel-containing steel alloy (9 % Ni). Because of this steel alloy, the inner layer tank exhibits excellent low-temperature resistance, good weldability and low susceptibility to cold cracks [3, 26]. As shown in Fig. 1, the inner tank consists of six different layers with a height of 8 m.

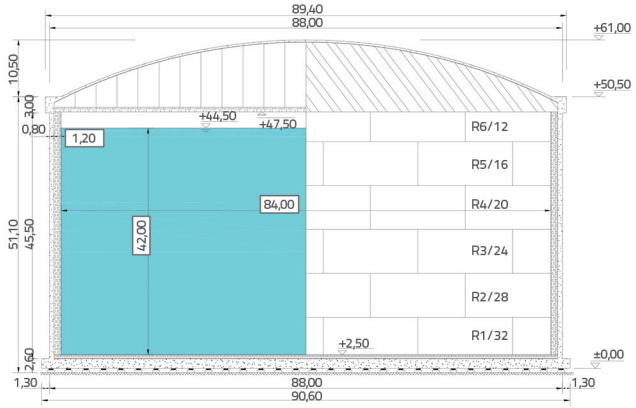

Figure 1. Schematic view of the basic design section of the liquefied natural gas (LNG) storage tank with a volume of 232,000 m³

For example, the R1/32 Layer refers to the first layer with a thickness of 32 mm at the bottom. The thicknesses of these layers gradually increase from top to bottom, as presented in Table 3. When the inner tank is filled with 100 % LNG, the maximum stress in it exceeds 500 MPa in the four site classes. Considering that the yield strength of the alloy steel used is between 500 and 600 MPa, this stress value poses a risk to structural safety [26, 31]. The selected LNG tanks were modelled using the ANSYS Workbench finite element program [32]. The outer and inner shells as well as the dome and foundation plate were modelled with four-point, 24-DOF rectangular shell elements. The fibre glass and pearlite isolation layers were modelled using eight-nodded 12-DOF solid elements. The fluid content was modelled using eight-nodded 12-DOF fluids. The fluid–structure interaction was approximated by determining the appropriate coupling equations at the nodes of the fluid–structure interface. The outer concrete wall, inner steel tank, concrete dome and ring beam, foundation slab, bottom foam glass and side perlite insulation were modelled using quadrilateral shell elements. In the analyses, the fluid side was considered an acoustic element and was combined with the structural side with the combining option to obtain results consistent with the theoretical calculations.

Table 3. Thickness of each layer in the inner tank

Layer	Level [m]	Height [m]	Thickness [mm]
1	+2.50 to +10.50	8.00	32
2	+10.50 to +18.50	8.00	28
3	+18.50 to +25.50	8.00	24
4	+25.50 to +33.50	8.00	20
5	+33.50 to +41.50	8.00	16
6	+41.50 to +47.50	5.00	12

The seismic analysis FEM developed in ANSYS Workbench was converted to LS-DYNA and seismic transient nonlinear analyses were carried out in LS-DYNA. The shell and solid elements had similar DOFs and types. The MAT_24 piecewise multilinear material model was used for the metal parts and the MAT_01 elastic model was adopted for the concrete and isolation parts. For the fluid side, MAT_NULL with Lagrangian options was used with automatic node-to-surface coupling of the sloshing effects have been presented.

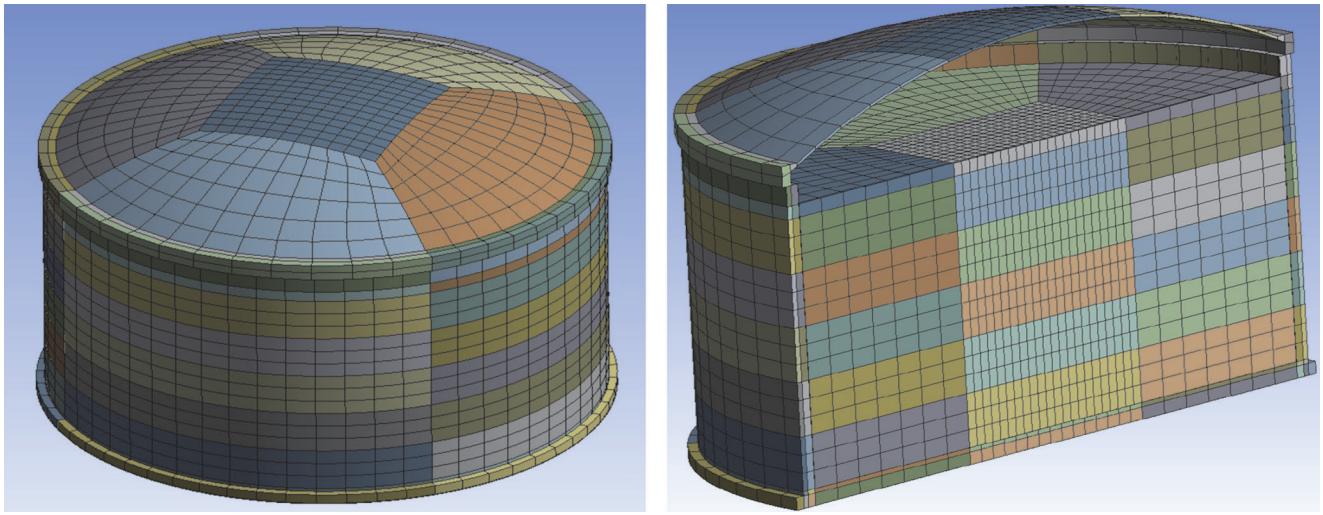

Figure 2. Finite element network structure for the LNG tank system

3. Modelling of the isolation systems

The base isolation systems used in this study included a series of similar rubber bearings homogeneously distributed under the foundation slab. The total number of required supports was calculated considering that a single element supports a maximum of 10 to 12 m^2 of foundation slab area [20, 21]. As this study aimed to examine the behavioural differences of isolator types under the same system, combined isolator placement was not performed. Therefore, the estimated number of bearings for a tank with a volume of 232,000 m^3 was 597. The frequency for extra-large LNG tanks is generally between 2 and 10 Hz, which is the specific resonance range for earthquake-induced ground movements [18].

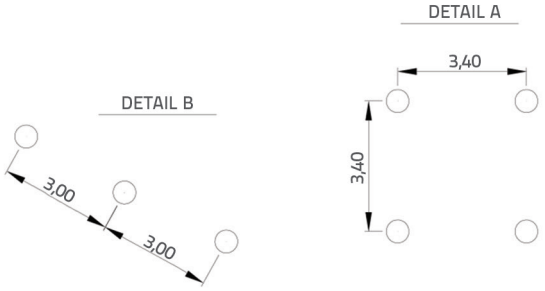

Figure 3. Details A and B

An FEM of the previously described LNG tank was developed to introduce seismic isolators at the base of the structure during the modal analyses. The bearings are assumed to have infinite vertical stiffness. Based on this assumption, the displacement constraint in the direction of the earthquake motion at the base of the tank walls was relaxed and nonlinear horizontal springs were placed to connect the base of the walls to the ground. In the ANSYS Workbench program, link elements (LINK8) that act as truss elements and combine nonlinear materials were used to model the seismic isolation system [32]. Using the SpaceClaim program, the bearings were converted to beam/link elements to maintain proper locations and the connection points were linked to the concrete base to create bonding. In the ANSYS Workbench program, it was assumed that the link elements were rigidly connected to the concrete and a fixed boundary condition was applied on the other side. For the seismic simulations, these link elements were converted to bushing elements using Beam ELFORM 6. The beam elements in LS-DYNA were MAT_197_SEISMIC_ISOLATOR, whose characteristics are described below..

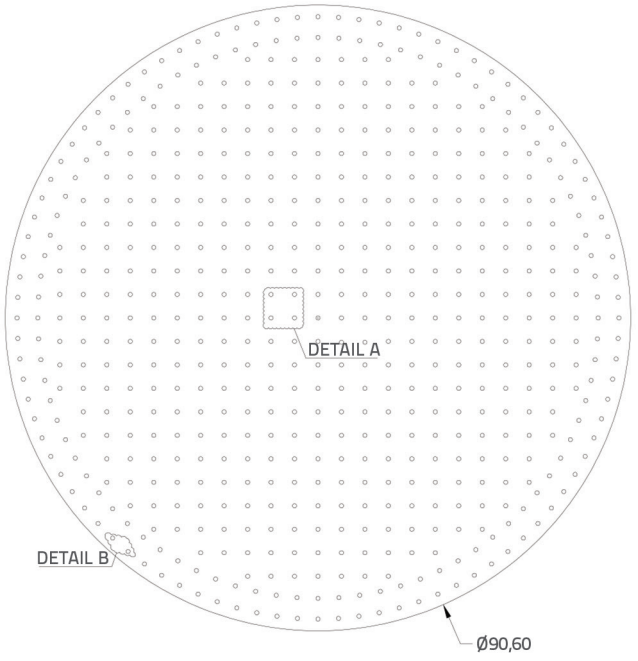

Figure 4. Earthquake isolation arrangement plan for high-damping rubber bearing (HDRB), lead-core rubber bearing (LRB) and friction pendulum system (FPS) isolators

Table 4. Engineering characteristics and bilinear spring parameters of HDRB SI-N 900/204 and LRB SI-N 900/225-185

Description	HDRB SI-N 900/204	LRB SI-N 900/225-185
Vertical stiffness K_v [kN/mm]	2317	2198
Effective horizontal stiffness K_e [kN/mm]	2.50	2.47
Elastic horizontal stiffness K_1 [kN/mm]	19.67	17.33
Yield displacement d_1 [mm]	12	18
Plastic horizontal stiffness K_2 [kN/mm]	1.97	1.77
Maximum seismic displacement d_2 [mm]	400	400
Maximum vertical load at load combinations including the seismic action [kN]	7980	6630
Elastomer stiffness [mm]	900	900
Elastomer thickness t_e [mm] of total design	204	225
Dynamic shear modulus G_{din} na γ =1 [MPa]	0.8	0.6

Table 5. Engineering characteristics and bilinear spring parameters of FPS FIP-D M 1600/800 (3700)

Description	FIP-D M 1600/800 (3700)
Vertical stiffness K_v [kN/mm]	36715
Restoring stiffness K_r [kN/mm]	0.6376
Effective horizontal stiffness K_e [kN/mm]	1.145
Friction force developed by the isolator F_0 [kN]	203.5
Maximum horizontal force F_{max} [kN]	458
Minimum friction coefficient μ [%]	4.872
Effective viscous damping ratio ξ_e	0.2826
Equivalent radius of curvature R [mm]	3700
Maximum seismic displacement d [mm]	400
Isolator diameter excluding anchoring elements D [mm]	940
Isolator height excluding dowels H [mm]	199

3.1. High damping rubber bearings (HDRB)

HDRBs are one of three main subtypes of steel-reinforced elastomeric bearings [33]. They consist of thin rubber layers reinforced with steel plates. According to a preliminary design [34], the number of high damping rubber bearings (SI-N 900/204) that should be used for an LNG tank with a volume of 232,000 m³ is 597. The properties used in this study are listed in Table 4.

3.2. Lead core rubber bearings (LRB)

Lead-core rubber bearings are composed of steel plate layers, rubber layers and a lead core. Similar to the steel shims in natural rubber bearings, the steel layers provide vertical stiffness, the rubber layers provide high lateral flexibility and the lead core provides these devices with extra stiffness and damping properties. According to a preliminary design [34], the number of lead core rubber bearings (SI-N 900/225-185) that should be used for an LNG tank with a volume of 232,000 m³ is 597. The properties used in this study are listed in Table 4.

3.3. Friction pendulum system (FPS)

Friction pendulum bearings are curved surface sliding bearings consisting of an articulated slider and a cover plate. The slider used in the system is covered with a self-lubricating composite liner. During an earthquake, the articulated slider on the bearing side along the concave surface enables the structure to move with gentle pendulum movements. According to a preliminary design [34], the number of the friction pendulum bearings [FIP-D M 1600/800 (3700)] that should be used for an LNG tank with a volume of 232,000 m³ is 597. The properties used in this study are listed in Table 5.

Table 6. Earthquake specifications used for the time history analyses

No	Earthquake ground motions (PEER register number)	Station	Abbrev.	Year	M_w	Time [s]	SSE scale factor	PGA (SSE)
1	Imperial Valley / SAD (RSN6)	El Centro Array	IV2	1940	6.95	53.72	4.85	1.022
2	Kern County / SAD (RSN15)	Taft Lincoln School	KC	1952	7.36	54.35	5.75	1.037
3	Borrego Mtn / SAD (RSN36)	El Centro Array	BM	1968	6.80	79.99	7.20	0.414
4	Imperial Valley-I / SAD (RSN162)	Calexico Fire Station	IV06-1	1979	6.53	37.86	6.30	1.282
5	Imperial Valley-II / SAD (RSN169)	Delta	IV06-2	1979	6.53	70.00	3.95	0.931
6	Victoria / Meksiko (RSN266)	Chihuahua	VM	1980	6.33	27.00	4.50	0.679
7	Irpinia / Italija (RSN286)	Bisaccia	IITA	1980	6.90	38.26	5.05	0.482

4. Analysis results

4.1. Earthquake ground motions

Analyses of the LNG tank system and the filling systems added to this system were conducted for three types of seismic ground motions: OBEs, SSEs and ALEs. According to the definitions in API 625 [4] and NFPA 59A [5] the ground motion of the OBE is represented by an acceleration response spectrum with a 10 % probability of deflection over a 50-year period (an average return interval of 475 years). An SSE is defined as the ground motion of an accepted maximum earthquake (MCE_R) over a 50-year period (mean recurrence interval of 2475 years) based on site-specific research. The ALE ground motion is defined as half of the SSE. The magnitudes used for the analyses of past earthquakes are given in Table 6, including the year, time, scale factor of the SSE, peak ground acceleration of the SSE and ground motion. A linear scaling approach was used to match the acceleration time series during the period of interest. The specified period range was selected as 0.1 and 12 s. This range represents a very broad spectrum band that matches the target acceleration spectrum, owing to the long agitation period (Tc_1 = ~9.7 s) of the stored LNG. Seven pairs of earthquake ground motions, called initial or core, were used to match the SSE spectrum. The calculations indicated that the impulsive mode of the median spectral coordinates matched well with the design spectrum for the specified periods, whereas the convective mode was significantly lower than the design spectrum for these periods. The adopted soil class was D and the ground motion and design level acceleration parameter values were determined as S_s = 1.926, S_1 = 0.660, S_{DS} = 1.926 (SSE) and S_{D1} = 1.123 (SSE). Seven pairs of earthquake ground motions were used as seeds to match the SSE spectra.

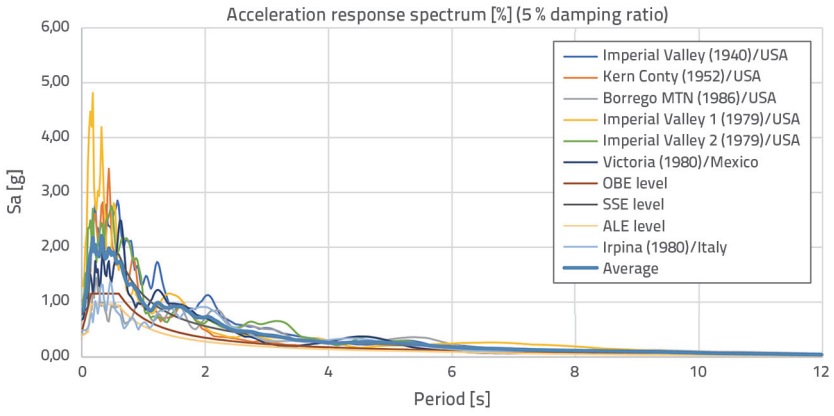

Figure 5. Acceleration site-specific response spectra for the design earthquake increased with the safe shutdown earthquake (SSE) scale factor

4.2. Modal analysis results

4.2.1. Inner steel tank and LNG fluid

The results of the inner steel tank and LNG fluid modal analyses for the non-isolated (anchored bottom) tank and systems with HDRB, LRB and FPS isolators are listed in Table 7. Figure 6 shows the first, second, third and fourth convective modes of the FEM. The convective mode shapes represent the agitation of the liquid in the tank without the tank wall. The impulsive mode shapes represent the combined motion of the tank and liquid. Figure 7 shows the first, second, third and fourth impulsive modes of the FEM.

The results of static and dynamic analyses of the LNG tank are presented in this section. The first horizontal convective and impulsive mode periods were 10 and 0.2302 s, respectively. The high-period (low-frequency) convective mode caused the agitation of the liquid and damaged the tank roof. The difference between the impulsive and convective mode frequencies indicated that the interaction effects between these modes were not significant.

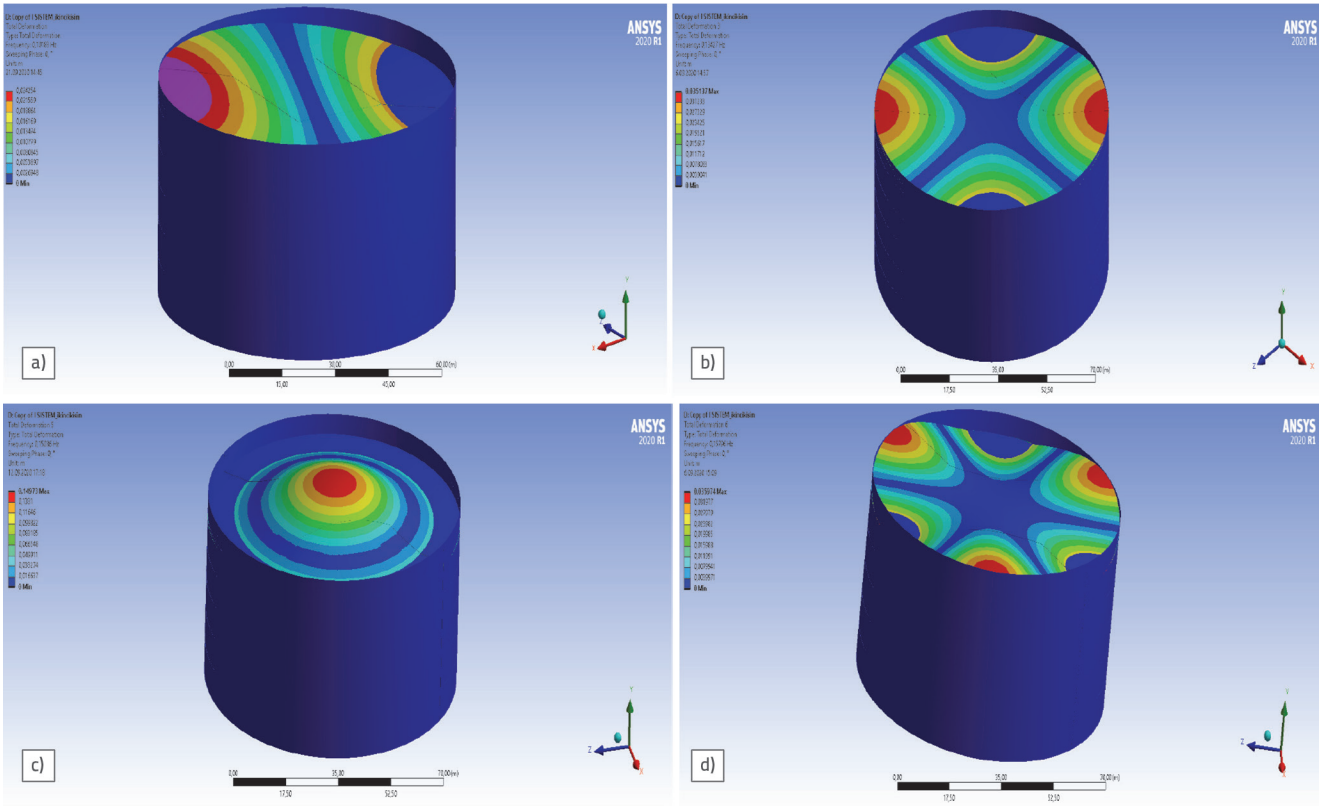

Figure 6. Convective mode types of the finite element model (FEM) for the non-isolated LNG tank: a) First convective mode T_1 = 9.8232 s; b) Second convective mode T_2 = 7.4460 s; c) Third convective mode T_3 = 6.6269 s; d) Fourth convective mode T_4 = 6.3291 s

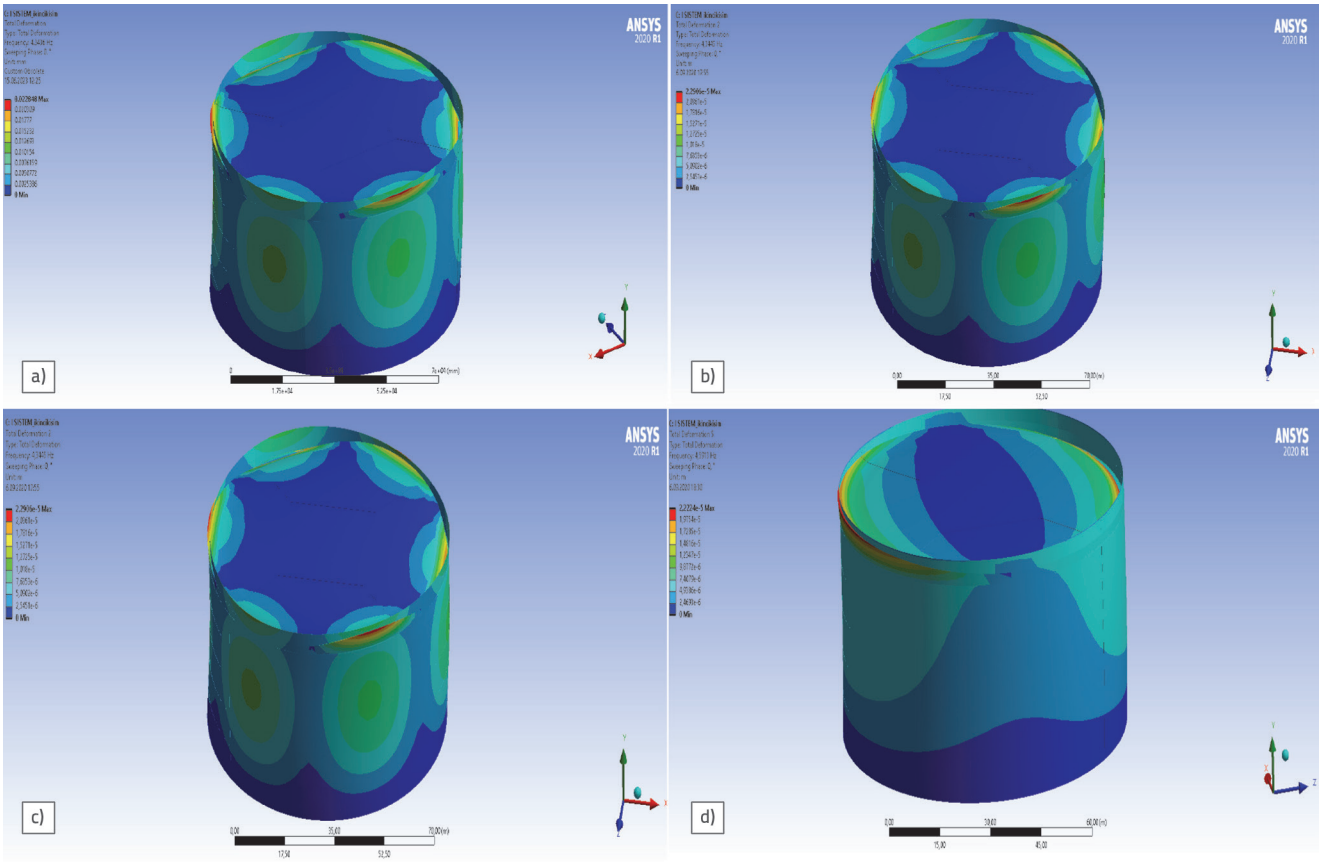

Figure 7. Impulsive mode types of the FEM for the non-isolated LNG tank: a) First impulsive mode T_1 = 0.2302 s; b) Second impulsive mode T_2 = 0.2301 s; c) Third impulsive mode T_3 = 0.2178 s; d) Fourth impulsive mode T_4 = 0.2158 s

Table 7. Natural periods of the inner model

Part	Mode number	Non-isolated		HDRB isolator		LRB isolator		FPS isolator	
		Frequency [Hz]	Period [s]	Frequency [Hz]	Period [s]	Frequency [Hz]	Period [s]	Frequency [Hz]	Period [s]
LNG Fluid	Mod 1	0.1018	9.8232	0.1011	9.8912	0.1011	9.8912	0.1006	9.9404
	Mod 2	0.1343	7.4460	0.1343	7.4460	0.1343	7.4460	0.1343	7.4460
	Mod 3	0.1509	6.6269	0.1509	6.6269	0.1509	6.6269	0.1509	6.6269
	Mod 4	0.1580	6.3291	0.1580	6.3291	0.1580	6.3291	0.1580	6.3291
	Mod 5	0.1780	5.6180	0.1780	5.6180	0.1780	5.6180	0.1780	5.6180
	Mod 6	0.1784	5.6054	0.1782	5.6117	0.1782	5.6117	0.1781	5.6148
Steel tank and LNG fluid	Mod 1	4.3436	0.2302	3.9718	0.2518	3.9706	0.2519	3.4718	0.2880
	Mod 2	4.3445	0.2301	4.0986	0.2440	4.0975	0.2441	3.8823	0.2576
	Mod 3	4.5913	0.2178	4.1754	0.2395	4.1741	0.2396	3.9885	0.2507
	Mod 4	4.633	0.2158	4.7762	0.2094	4.7417	0.2109	4.099	0.2440
	Mod 5	5.016	0.1994	5.0602	0.1976	5.0593	0.1977	4.8246	0.2073
	Mod 6	5.301	0.1886	5.7193	0.1748	5.7174	0.1749	5.010	0.1996

4.2.2. Outer concrete

Modal analyses were also performed for the external prestressed concrete walls, ring beams, domes and mat foundations. The results of the outer concrete modal analyses for the non-isolated tank and systems with HDRB, LRB and FPS isolators are listed in Table 8. Figure 8 shows the first, second and third mode shapes of the FEM. In the first mode,

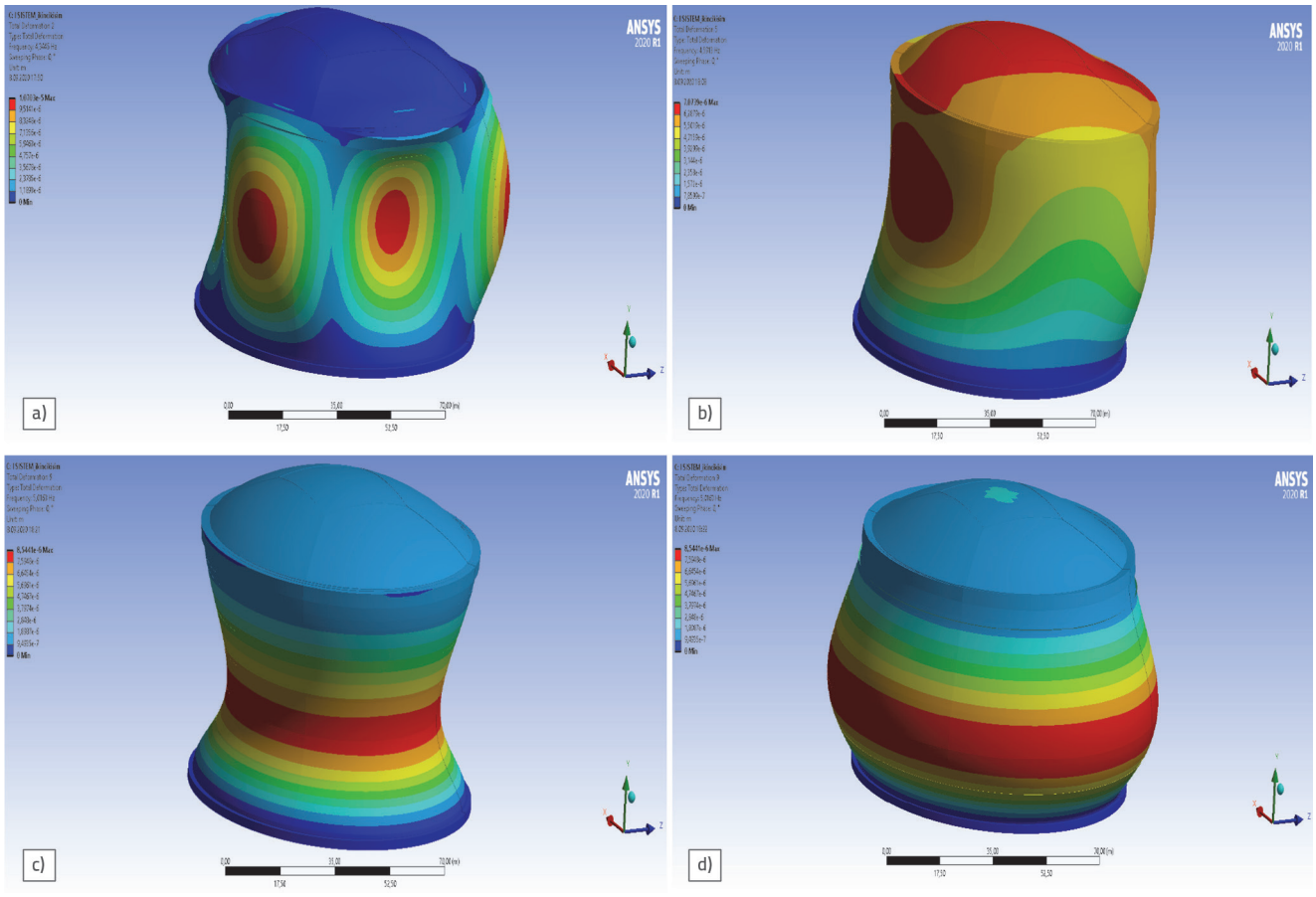

Figure 8. Outer concrete mode shapes of the FEM for the non-isolated tank: a) First mode T_1 = 0.2302 s; b) Second mode T_2 = 0.2178 s; c) Third mode T_3 = 0.1994 s

Table 8. Natural periods of the outer concrete model

Part	Mode No	Non-isolated		HDRB isolator		LRB isolator		FPS isolator	
		Frequency [Hz]	Period [s]	Frequency [Hz]	Period [s]	Frequency [Hz]	Period [s]	Frequency [Hz]	Period [s]
Outer concrete tank	Mod 1	4.3445	0.2302	3.9718	0.2518	3.9716	0.2518	3.4718	0.2880
	Mod 2	4.5913	0.2178	4.7762	0.2094	4.7174	0.2120	3.8823	0.2576
	Mod 3	5.0163	0.1994	5.7193	0.1748	5.7174	0.1749	4.8246	0.2073

the walls were deformed in the radial direction; however, the roof diaphragm did not move laterally. In the second mode, the walls were displaced laterally, whereas the ring beam, dome and foundation were rigid. In the third mode, the prestressed concrete walls moved along their axes in the positive and negative directions.

4.3. Times history analysis results

The ground motion acceleration was defined using the LOAD_BODY_X option in the LS-DYNA program. The ground was fixed to provide the structure with inertia. Additionally, LOAD_BODY_Z was defined to conserve gravity. Because a large structure with a fluid domain was analysed, an inclined interface time was used to neglect the initial gravitational effect and avoid unnecessary strain on the structure. The LS-DYNA software was used to simulate the fluid–structure interaction in a tank filled with fluid. This software offers significant advantages, particularly for solving dynamic contact problems. In addition, the LS-DYNA program provides materials and standardised contact formulations that can be used to model fluids and represent the interaction between the tank shell and fluid during seismic excitation.

4.3.1. Inner steel tank stresses

The inner tank maximum von Mises stress values (MPa) and percentages (%) of reduction with respect to the non-isolated values occurring during a seven-scale earthquake in the non-isolated and HDRB-, LRB- and FPS-isolated LNG tanks fully filled with LNG are given in Table 9. The maximum stress distributions of the non-isolated and HDRB-, LRB- and FPS-isolated LNG tanks for the 1940 Imperial Valley Earthquake El Centro Array Base Station data are shown in Fig. 9. Compared with conventional tanks, HDRB, LRB and FPS seismic isolators provide an average reduction of 15 % to 5 % in repulsive modes. Considering the fixed base

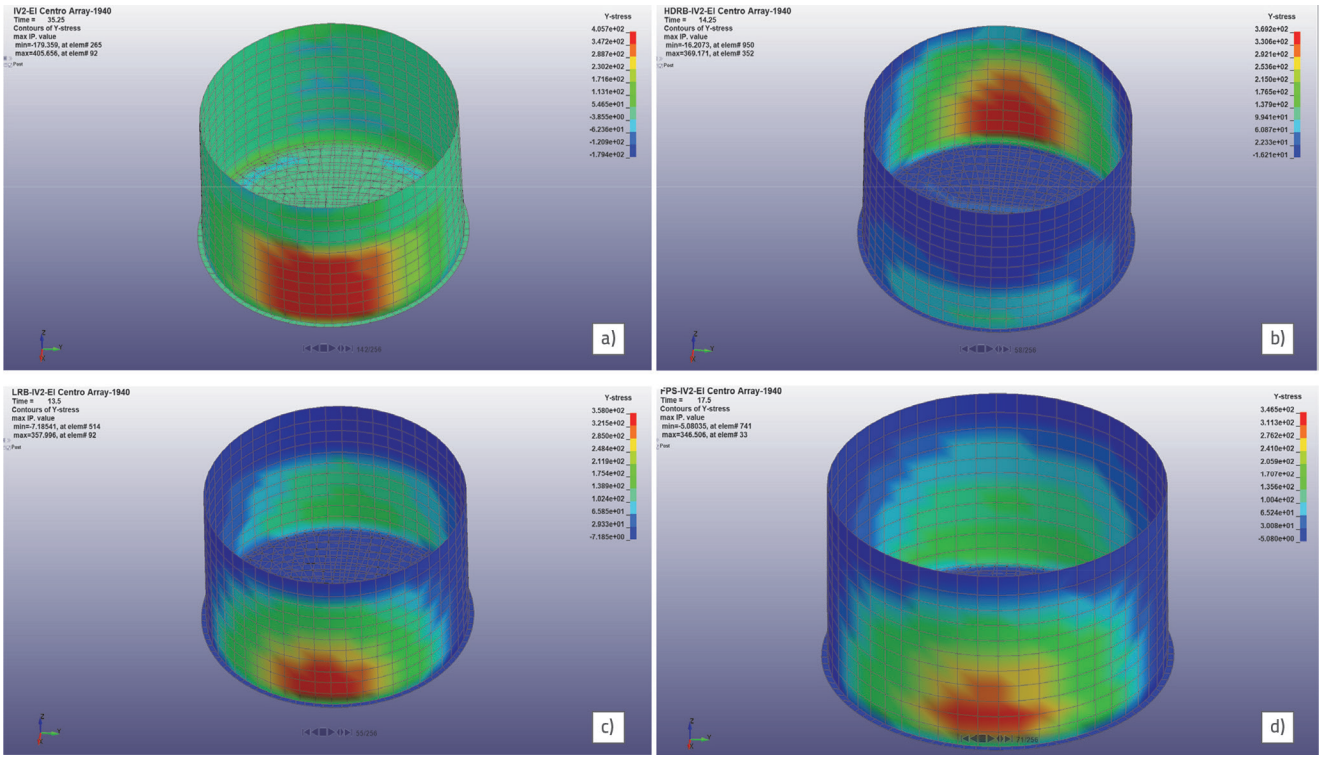

Figure 9. Inner steel tank wall tension stresses for non-isolated and HDRB-, LRB- and FPS-isolated tanks: a) Non-isolated; b) HDRB isolator; c) LRB isolator; d) FPS isolator

Table 9. Inner tank maximum von Mises stress values (MPa) and reduction rates (%) with respect to the non-isolated values

Earthquake ground motions	Base type						
	Non-isolated	HDRB isolator		LRB isolator		FPS isolator	
IV2-1940	406	369	9 %	358	12 %	347	15 %
KC-1952	378	354	6 %	354	6 %	349	8 %
BM-1968	380	348	8 %	348	8 %	346	9 %
IV06-I-1979	392	357	9 %	346	12 %	350	11 %
IV06-II-1979	405	348	14 %	355	12 %	345	15 %
VM-1980	382	352	8 %	352	8 %	345	10 %
IITA-1980	375	351	6 %	356	5 %	328	12 %

conditions, the reduction in the maximum stresses in the inner shell of approximately 15 % compared with the non-isolated situation reveals the importance of isolator use. Dynamic loads generate much greater stress than static loads, which is critical for LNG tanks. Considering that the yield strength of 9 % Ni steel is between 515 MPa and 585 MPa, the maximum stress in the inner tank of the anchored LNG tank exceeding 400 MPa poses a risk to the safety of the structure [26, 31].

4.3.2. LNG fluid maximum sloshing wave height

The LNG fluid maximum sloshing wave height values (mm) and percentages (%) of reduction with respect to the non-isolated values occurring during a seven-scale earthquake in the non-isolated and HDRB-, LRB- and FPS-isolated LNG tanks fully filled with LNG are given in Table 10. The maximum sloshing wave heights of the non-isolated and HDRB-, LRB- and FPS-isolated LNG tanks for the 1979 Imperial Valley earthquake Calexico Fire Station data are shown in Fig. 10. The FPS and LRB earthquake isolators exhibited the best performance at the height of the agitated liquid in the LNG tank, which was examined for seven different earthquakes and four different systems. This result can be explained by a friction force of approximately 200 kN when the FPS-type earthquake isolator was used. This frictional force absorbs the horizontal forces that occur during an earthquake. In an LRB-type isolator, the lead core in the centre absorbs horizontal forces. Higher sloshing heights than those in the LRB, FPS and fixed-bottom LNG tanks were observed when the HDRB-type isolator was used. The LNG tank oscillated because of the horizontal force originating

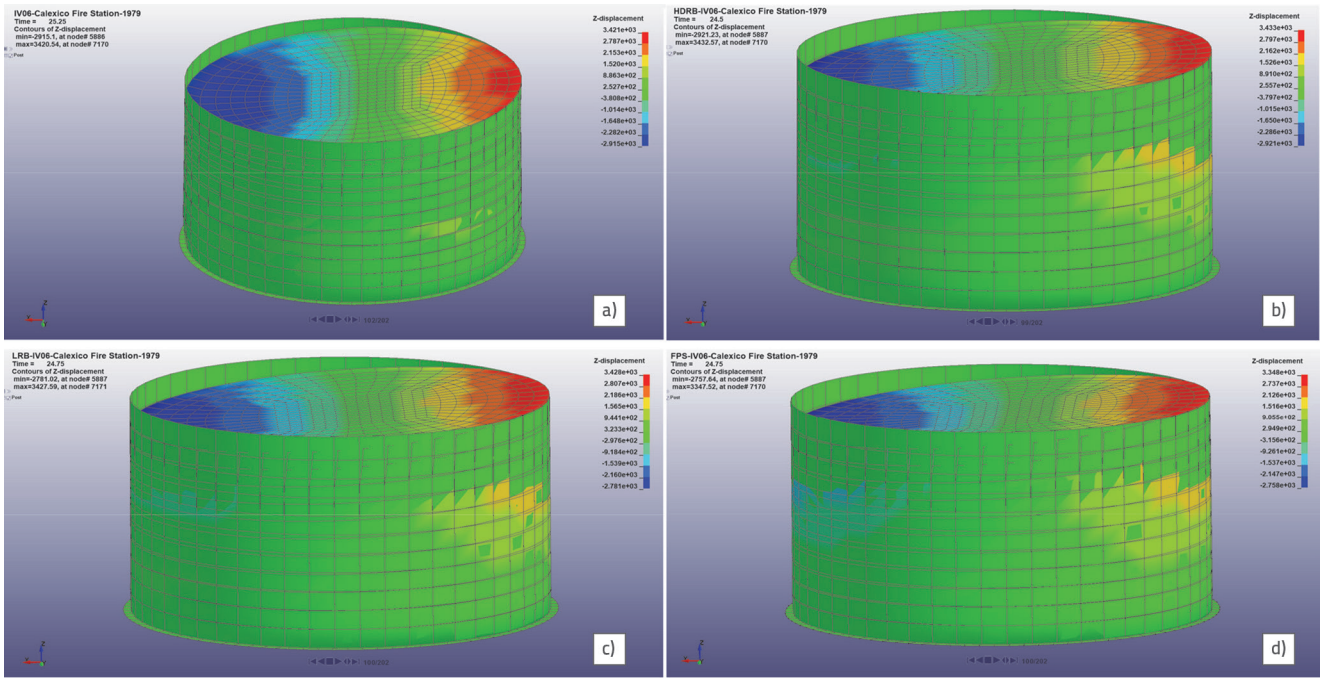

Figure 10. LNG fluid maximum sloshing wave height for non-isolated and HDRB-isolated, LRB-isolated and FPS-isolated tanks: a) Non-isolated; b) HDRB isolator; c) LRB isolator; d) FPS isolator

Table 10. LNG fluid maximum sloshing wave height values (mm)

Structural bearing type	IV2-1940	KC-1952	BM-1968	IV06-I-1979	IV06-II-1979	VM-1980	IITA-1980
Fixed	2463	2119	3317	3421	2006	2567	3355
HDRB	2577	1920	3638	3433	1959	2836	3488
LRB	2379	1934	3560	3428	1880	2470	3438
FPS	2090	1932	3550	3348	1899	2760	3276

from the rubber system. As a result, the LNG liquid height in the convective mode increased during an earthquake. The sloshing height in conventional tanks was higher than that in LNG tanks with isolators in the Kern County and Imperial Valley-II earthquakes and the earthquake oscillations in the convective mode continued with high accelerations.

4.3.3. The maximum lateral displacement of inner steel tank wall

The maximum lateral displacement values (mm) and reduction rates (%) of the inner steel tank with respect to the non-isolated values occurring during a seven-scale earthquake in the non-

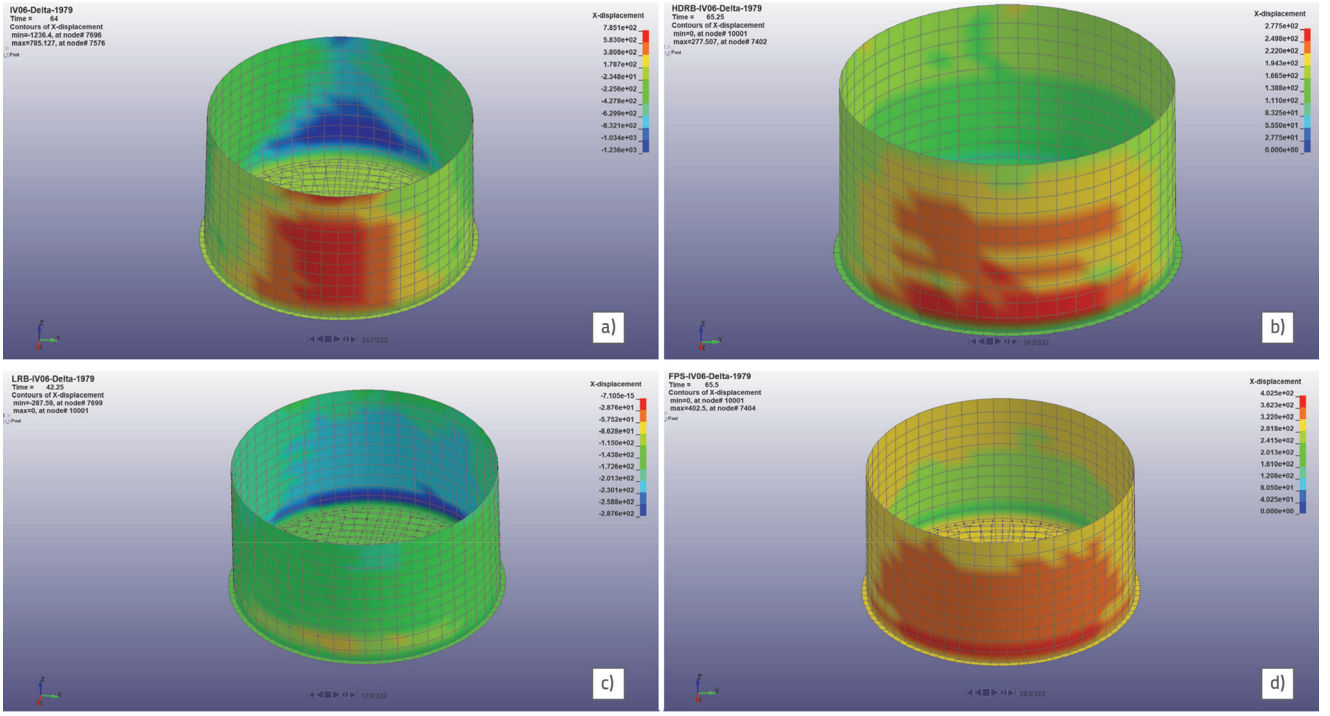

Figure 11. Maximum lateral displacement values (mm) at the steel wall for non-isolated and HDRB-, LRB- and FPS-isolated tanks: a) Non-isolated; b) HDRB isolator; c) LRB isolator; d) FPS isolator

Table 11. Maximum lateral displacement values (mm) at the steel tank wall and reduction rates (%) with respect to the non-isolated values

Earthquake ground motions	Base type						
	Non-isolated	HDRB isolator		LRB isolator		FPS isolator	
IV2-1940	898	496	45 %	424	53 %	604	33 %
KC-1952	578	361	38 %	369	36 %	329	43 %
BM-1968	369	322	13 %	278	25 %	345	7 %
IV06-I-1979	706	553	22 %	430	39 %	299	58 %
IV06-II-1979	1120	287	74 %	287	74 %	401	64 %
VM-1980	449	444	1 %	312	30 %	440	2 %
IITA-1980	171	263	-53 %	253	-48 %	297	-74 %

isolated and HDRB-, LRB- and FPS-isolated LNG tanks fully filled with LNG are given in Table 11. The maximum lateral displacements of the inner steel tank wall values of the non-isolated and HDRB-, LRB- and FPS-isolated LNG tanks for the 1979 Imperial Valley Earthquake Delta Station data are shown in Fig. 11. It was observed that the horizontal displacement movements of the inner tanks in the isolated LNG tank were less than those of the fixed system during high-acceleration and long oscillating earthquakes. However, the elephant foot deformation type, which is observed in low-intensity earthquakes, is less common in LNG tanks fixed to the foundation with anchor bolts than in structures with isolators. When using an LRB-type isolator in severe earthquakes, less lateral deformation occurs in the inner tank compared with that generated with other isolator systems. This is because of the ability of the lead core in the centre of the LRB-type isolators to inhibit lateral displacement.

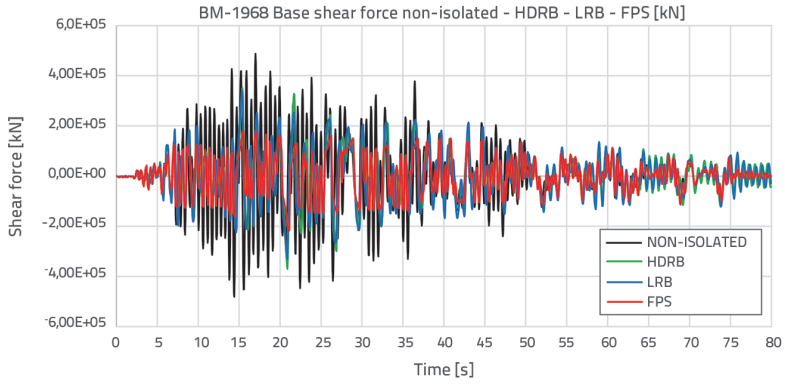

Figure 12. LNG tank base shear force non-isolated and HDRB-, LRB- and FPS-isolated tanks

4.3.4. Maximum base shear force of inner steel tank

The maximum base shear forces of the inner steel tank (kN) and reduction rates (%) with respect to the non-isolated values occurring during a seven-scale earthquake for non-isolated and HDRB-, LRB- and FPS-isolated LNG tanks fully filled with LNG are given in Table 12. The maximum base shear force values of the non-isolated and HDRB-, LRB- and FPS-isolated LNG tanks for the 1979 Imperial Valley earthquake Delta Station data are shown in Fig. 12. The maximum base shear forces of the inner steel tank for the HDRB and LRB isolator systems were between 50 % and 10 % lower than those of the non-isolated LNG tanks. It has been observed that the base shear forces formed in LNG tanks with an FPS are 67 %–49 % lower than those in systems without isolators. Because systems with FPS operate according to the friction principle, the base shear forces that occur in these systems during an earthquake are less than those of the LRB and HDRB isolator systems. Consequently, LNG tanks with friction-based pendulum-type isolators performed much better than other rubber-based isolator systems when compared to the base shear forces occurring during earthquakes.

The comparative analysis results of the maximum inner steel tank von Mises stresses, LNG fluid sloshing wave heights, inner steel tank lateral displacements and base shear forces are shown in Fig. 13.

4.3.5. Force–displacement diagrams for LNG isolation types

The force (kN) and displacement (mm) values during a seven-scale earthquake for the HDRB-, LRB- and FPS-isolated LNG tanks fully filled with LNG are listed in Table 13. The force–displacement graphics of the LNG tank base isolators of the HDRB-, LRB- and FPS-isolated LNG tanks for the 1940 Imperial Valley earthquake El Centro Array Base Station data are shown in Fig. 14. While the LRB earthquake isolator shows less displacement than the other isolators under the effect of a large shear force coming from the LNG tank in high-acceleration and long-oscillating earthquakes,

Table 12. Maximum base shear forces (kN) and reduction rates (%) with respect to the non-isolated tanks for HDRB-, LRB- and FPS-isolated tanks

Earthquake ground motions	Base type						
	Non-isolated	HDRB isolator		LRB isolator		FPS isolator	
IV2-1940	6.78×10^5	5.26×10^5	22 %	4.48×10^5	34 %	3.10×10^5	54 %
KC-1952	5.92×10^5	3.98×10^5	33 %	3.94×10^5	34 %	2.08×10^5	65 %
BM-1968	4.87×10^5	3.70×10^5	24 %	3.38×10^5	31 %	2.18×10^5	55 %
IV06-I-1979	6.08×10^5	5.47×10^5	10 %	4.33×10^5	29 %	2.01×10^5	67 %
IV06-II-1979	6.44×10^5	3.19×10^5	50 %	3.27×10^5	49 %	2.36×10^5	63 %
VM-1980	6.29×10^5	4.72×10^5	25 %	3.56×10^5	43 %	2.53×10^5	60 %
IITA-1980	3.89×10^5	3.21×10^5	17 %	3.09×10^5	21 %	1.97×10^5	49 %

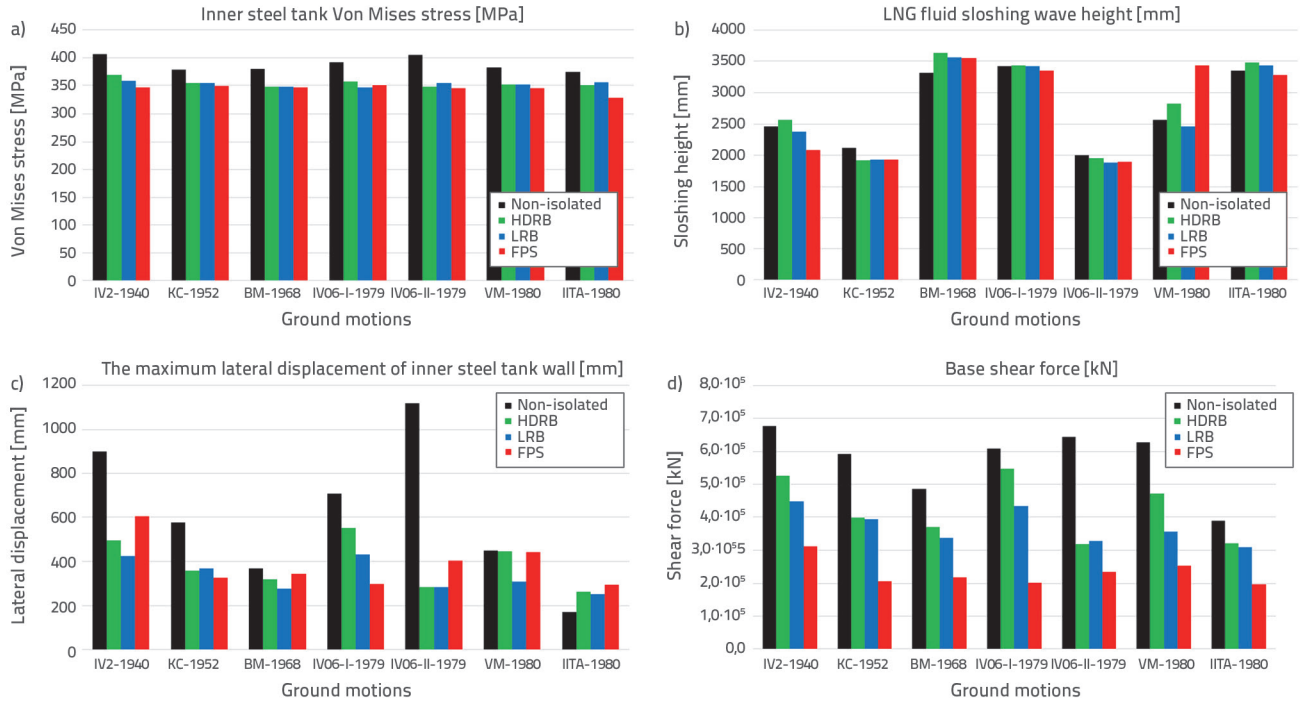

Figure 13. Nonlinear analysis results: a) Von Mises stress (MPa); b) sloshing wave height (mm); c) lateral displacement (mm); d) base shear force (kN)

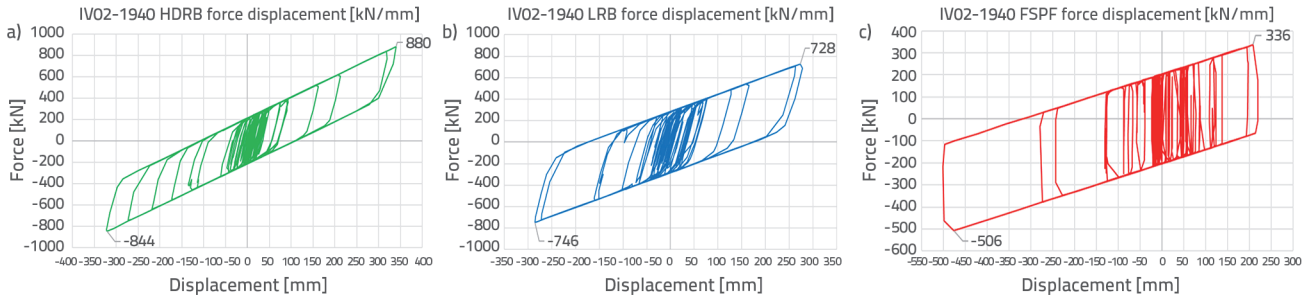

Figure 14. LNG tank base isolators force–displacement graphics:) HDRB isolator; b) LRB isolator; c) FPS isolator

Table 13. LNG tank base isolators maximum force–displacement values

Earthquake ground motions	Isolator type					
	HDRB		LRB		FPS	
	Force [kN]	**Displacement** [mm]	**Force** [kN]	**Displacement** [mm]	**Force** [kN]	**Displacement** [mm]
IV2-1940	880	340	746	286	506	499
KC-1952	656	225	658	232	345	229
BM-1968	615	205	564	173	363	256
IV06-I-1979	904	360	710	274	336	210
IV06-II-1979	534	164	544	164	395	302
VM-1980	791	296	595	194	422	346
IITA-1980	536	165	518	145	328	195

the FPS isolators perform better in moderate-intensity and low-oscillation earthquakes. This is because the horizontal displacement force–displacement angle ratio of the LNG tank in earthquakes when FPS-type isolators are used and the friction-damped force is exceeded is higher than that with LRB- and HDRB-type isolator systems. Compared to the HDRB isolator system, the lead in the LRB core limited the horizontal displacement movement of the LNG tank. The horizontal displacement of LNG tanks during an earthquake is critical because of the mechanical and carrier pipe systems; in this respect, the LRB isolator type is more advantageous than the FPS and HDRB.

5. Conclusions

In this study, an LNG tank with a volume of 232,000 m^3 placed on four different base types was analysed under seven different earthquake effects. The height-to-radius ratio was selected as 1 for maximum LNG fluid. The base shear force, sloshing height, inner steel tank lateral deflection, von Mises stresses in the inner steel tank and force–displacement of the isolators were investigated.

- When comparing the LNG tanks with the HDRB, LRB and FPS isolators with that fixed to the foundation with anchor bolts, no difference was observed between the convective and impulsive modes. It was concluded that the wave motion of the liquid was different from the oscillation of the structure and the earthquake isolation times did not affect the sloshing motion.
- An average stress of 270 MPa occurred in the inner steel tank owing to the static loading. The stresses varied depending on the intensity of the earthquake and whether the system was isolated or fixed. While a stress value of 400 MPa occurred in the fixed system, these values were 350 MPa on average for the LNG tanks with the HDRB, LRB and FPS-type earthquake isolator systems. The yield strength of the steel tank is between 515 and 585 MPa. According to the API 620 standard, 80 % of this value (412–468 MPa) should not be exceeded for the SSE. Otherwise, there is a significant risk to LNG tanks. Therefore, base isolator systems should be used in structures under risk.
- The sloshing time varies between 9.82–9.94 s for tanks without isolator and with HDRB-, LRB- and FPS-type isolators. For the isolated and anchored systems, the wave height varies depending on the agitation time of the LNG liquid. The sloshing wave height of the liquid is proportional to the harmonic movements of the earthquake acceleration of the structure rather than the numerical magnitude of the earthquake accelerations. For example, the sloshing wave height for acceleration values varying between +0.3 g and −0.3 g of the BM-1968 earthquake within a period of 10 s is greater than that for the IV06-II-1979 earthquake.
- Except for earthquakes such as IV06-I-1979 with very high acceleration values, the sloshing wave height observed as a result of the regular harmonic motion acceleration values formed in anchored LNG tanks was less than that in structures with isolators. This result can be attributed to the damping function oscillating between high and low acceleration values. However, the acceleration values decrease owing to the damping provided by the lead core in the LRB centre and the frictional force generated in the FPS, resulting in a lower sloshing height in tanks using these types of isolators than that in tanks with the HDRB isolator.
- In moderate and weak earthquakes, such as the Irpina earthquake, the pressure of the impulsive mass in the inner steel tank is blocked by the anchors and the lateral displacement movement of the structure is not allowed. This is why there is buckling with less movement than that in structures with isolators. However, in earthquakes of +0.4 g and above, the lateral displacement of the inner steel tank wall in the anchored LNG tank is greater than that in tanks with LRB, HDRB and FPS isolators. Therefore, elasto-plastic buckling of the inner steel tank, which we call the elephant foot strain, was observed in the anchored tanks.
- With an increase in average ground acceleration, the total bottom shear force acting on the LNG tank increased. Moreover, with an increase in the maximum shear force on the base, the percentage of shear force reduction in systems with isolators also increased. The bottom shear forces were found to be similar in the LNG tanks with HDRB and LRB isolators. However, better performance was obtained in LNG tanks with an FPS system compared with that of the other two isolator types. This can be attributed to the fact that each FPS isolator generated a frictional force that absorbed a base shear force of 200 kN.
- LNG transported by pipes from a ship docking at a port is discharged from the roof of the LNG tank to the inner steel tank. During this time, it is desirable that the horizontal displacement of the LNG tank be limited during an earthquake to avoid damage to the mechanical and piping systems. When the force–displacement graphs of the HDRB, LRB and FPS isolator-supported LNG tanks are examined, it can be observed that, compared with the other earthquake isolators, the LRB isolator has the least horizontal displacement. When the acceleration–time graphs of seven earthquakes with 0.4 g and above ground movements are examined, the FPS showed more lateral displacement than the HDRB and LRB LNG tanks because of the amount of horizontal force acting on each isolator. This can be attributed to the earthquake forces exceeding the friction-damped force and reaching a higher horizontal displacement motion. This situation is undesirable for LNG tanks. Meanwhile, the LRB system provides a 10 %–15 % advantage over the HDRB isolator owing to the horizontal damping of the middle lead core.

- It was observed that earthquake isolators used in LNG storage tanks perform well even during very strong earthquakes, which may occur once every 2475 years. The use of isolator systems is recommended for the earthquake safety of LNG storage tanks, as they may cause major environmental disasters and destruction. Systems with LRB isolators outperformed those with FPS and HDRB isolators and fixed support systems in all criteria, except for the base shear force.

Acknowledgments

This study was funded by the Pamukkale University Scientific Research Project Coordination Unit (grant number 2019FEBE055). The authors would like to thank to Associate Prof. Temel Varol from the Metallurgical and Materials Engineering Department, Karadeniz Technical University, Ph.D. student Murat Çelik from the Civil Engineering Department, Istanbul Technical University and M.Sc. Mechanical Engineer Hakan Balaban for their valuable contributions.

REFERENCES

[1] Marti, J., Crespo, M., Martinez, F.: Seismic isolation of liquefied natural gas tanks: A comparative assessment, The Journal of the Anti-Seismic Systems International Society, 1 (2010) 1, pp. 125-140, doi:10.2140/siaps.2010.1.125.

[2] Summers, P.B., Castellano, M.G., Bergamo, G., Gatti, F., Marti, J., Poggianti, A.: Seismic risk reduction at petrochemical and LNG acilities: Main results from in-depth project, 14th World Conference on Earthquake Engineering, Beijing, China, October, 2006.

[3] API Standard 620, Design and construction of large, welded, low-pressure storage tanks, American Petroleum Institute Publishing Services, 12th Edition, Addendum 1, API, Washington D.C., USA, 2014.

[4] API Standard 625, Tank systems for refrigerated liquefied gas storage, American Gas Association Publishing Services, 1st Edition, Addendum 2, AGA, Washington D.C., USA, 2014.

[5] NFPA 59A, Standard for the production, storage and handling of liquefied natural gas LNG, National Fire Protection Association Publishing Services, NFPA , Washington D.C., USA, 2016.

[6] Westergaard, H.M.: Water pressures on dams during earthquakes, Transactions of the American Society of Civil Engineers, 98 (1933) 2, Washington D.C., USA.

[7] Jacobsen, L.S.: Impulsive hydrodynamics of fluid inside a cylindrical tank and of fluid surrounding a cylindrical pier, Bulletin of the Seismological Society of America, 39 (1949) 3, pp. 189-204, doi:10.1785/BSSA0390030189.

[8] Jacobsen, L.S., Ayre, R.S.: Hydrodynamic experiments with rigid cylindrical tanks subjected to transient motions, Bulletin of the Seismological Society of America, 41 (1951) 4, pp. 313-346, doi:10.1785/BSSA0410040313.

[9] Housner, G.W.: Dynamic pressures on accelerated fluid containers, Bulletin of the Seismological Society of America, 47 (1957) 1, pp. 15-35, doi:10.1785/BSSA0470010015.

[10] Housner, G.W.: The dynamic behavior of water tanks, Bulletin of the Seismological Society of America, 1963, 53 (1963) 2, pp. 381-387, doi:10.1785/BSSA0530020381.

[11] Veletsos, A.: Seismic effects in flexible liquid storage tanks, in Proceedings of the 5th World Conference on Earthquake Engineering, Rome, Italy, June, 1974.

[12] Veletsos, A., Yang J.: Dynamics of fixed-base liquid storage tanks, in Proceedings of the US–Japan Seminar for Earthquake Engineering Research with Emphasis on Lifeline Systems, Tokyo, Japan, November, 1976.

[13] Haroun, M.A., Housner, G.W.: Dynamic interaction of liquid storage tanks and foundation soil, in Dynamic Response of Structures: Experimentation: Observation, Prediction and Control, American Society of Civil Engineers, ASCE, New York, USA, 1981.

[14] Veletsos, A.S., Tang, Y.: Soil-structure interaction effects for laterally excited liquid-storage tanks., Earthquake Engineering and Structural. Dynamics, 19 (1990) 4, pp. 473-496, doi:10.1002/eqe.4290190402.

[15] Malhotra, P.K., Wenk, T., Wieland, M.: Simple procedures for seismic analyses of liquid storage tanks, Structural Engineering International, 10 (2000) 3, pp. 197-201, doi:10.2749/101686600780481509.

[16] Zhao, Y., Li, H.N., Fu, X., Zhang, S., Mercan, O.: Seismic analyses of a large LNG tank considering the effect of liquid volume, Hindawi, (2020), Article ID 8889055, pp. 1-18, doi:10.1155/2020/8889055.

[17] Bomhard, H., Stempniewski, L.: LNG tanks for seismically highly affected sites, Intl. Post SMiRT Conference Seminar on Isolation, Energy Dissipation and Control of Vibrations of Structures, IAEA, Capri, Italy, 1993.

[18] Tajirian, F.F.: Base isolation design for civil components and civil structures, in Proceedings of the Structural Engineers World Conference, San Francisco, California, USA, July, 1998.

[19] Castellano, M.G., Infanti, S., Dumoulin, C., Ducoup, L., Martelli, A., Dusi, A.: Shaking table tests on a liquefied natural gas storage tank mock-up seismically protected with elastomeric isolators and steel hysteretic torsional dampers, 12th World Conference on Earthquake Engineering, Auckland, New Zealand, February, 1999.

[20] Gregoriou, V.P., Tsinopoulos, S.V., Karabalis, D.L.: Base isolated LNG tanks: Seismic analyses and comparison studies, First European Conference on Earthquake Engineering and Seismology, Geneva, Switzerland, September, 2006.

[21] Gregoriou, V.P., Tsinopoulos, S.V., Karabalis, D.L.: Dynamic analyses of liquefied natural gas tanks seismicly protected with energy dissipating base isolation systems, 3rd ECCOMAS Thematic Conference on Computational Methods in Structural Dynamics and Earthquake Engineering, Corfu, Greece, May, 2011.

[22] Ruifu, Z., Dagen W., Xiaosong, R.: Seismic analyses of a LNG storage tank isolated by a multiple friction pendulum system, Earthquake Engineering and Engineering Vibration, 10 (2011) 2, pp. 253-262, doi:10.1007/s11803-011-0063-3.

[23] Christovasilis, I.P., Whittaker, A.S.: Seismic analyses of conventional and isolated LNG tanks using mechanical analogs, Earthquake Spectra, 2008, 24 (2008) 3, pp. 599-616, doi:10.1193/1.2945293.

[24] Datoli, R., Danilo, B., Perillo, M.: Sloshing response of a LNG storage tank subjected to seismic loading, 6th European LS-DYNA Users' Conference, Gothenburg, Sweden, May, 2007.

[25] Zhou, Y., Li, X., Chen, Z.: Seismic responses analyses of base-isolated LNG storage tank, in Proceeding of GeoShanghai 2018 International Conference: Advances in Soil Dynamics and Foundation Engineering, Singapore, May, 2018.

[26] Zhou, Y., Li, H., Zhang S., Mercan, O., Caiyan, Z.: Seismic analyses of a large LNG tank considering different site conditions, Applied Sciences, 10 (2020) 22, pp. 8121, doi:10.3390/app10228121.

[27] Barone, S., Sartori, M.: Seismic isolation of LNG storage tanks in Italy with curved surface sliders, 17th World Conference on Earthquake Engineering, Sendai, Japan, September, 2020.

[28] Kılıç, S., Akbaş, B., Shen, J., Paolacci, F.: Seismic behavior of liquid storage tanks with 2D and 3D base isolation systems, Structural Engineering and Mechanics, 83 (2022) 5, pp. 627-644, doi:10.12989/sem.2022.83.5.627.

[29] Chen, Z., Xu, Z., Teng, L., Fu, J., Xu, T., Zhao, Z.: Experimental and numerical investigation for seismic performance of a large-scale LNG storage tank structure model, Applied Sciences, 12 (2022) 17, pp. 8390, doi:10.3390/app12178390.

[30] Sharari, N., Behzad, F., Hokmabadi A., Xu, R.: Seismic resilience of extralarge LNG tank built on liquefable soil deposit capturing soilpilestructure interaction, Bulletin of Earthquake Engineering, 20 (2022) 4, pp. 3385-3441, doi:10.1007/s10518-022-01384-1.

[31] Standardization Administration Committee of the People's Republic of China: 9 % Nickel Steel Plates for Pressure Vessels with Specified Low Temperature Properties, SAC, Beijing, China, 2010.

[32] ANSYS Workbench 20, LS-DYNA 2018, Southpointe, 275 Technology Drive, PA 15317, ANSYS Inc., Canonsburg, USA, 2022.

[33] Vaiana, N., Sessa, S., Marmo, F., Rosati, L.: An accurate and computationally efficient uniaxial phenomenological model for steel and fiber reinforced elastomeric bearings, Composite Structures, 211 (2019) 11, pp. 196-212, https://doi.org/10.1016/j.compstruct.2018.12.017.

[34] FIP MEC Srl., Via Scapacchio, 41/35030 Selvazzano Dentro, Italy, 2022.